

DIRECT MEASUREMENT OF TURBULENT PARTICLE EXCHANGE WITH A
TWIN CPC EDDY COVARIANCE SYSTEM

Andreas Held*, Otto Klemm

Bayreuth Institute of Terrestrial Ecosystem Research (BITÖK), University of Bayreuth,
95440 Bayreuth, Germany

Now at: Institute of Landscape Ecology (ILÖK), University of Münster, 48149 Münster,
Germany

* Corresponding author: Phone: +49-251-83-33923

Fax: +49-251-83-38352

andreas.held@uni-muenster.de

KEYWORDS

eddy covariance, particle deposition, deposition velocity, ultrafine particles, Norway spruce

ABSTRACT

Direct measurements of particle number fluxes by eddy covariance (EC) were carried out in the years 2001 and 2002 during the BEWA2000 field experiments. An EC system combining a sonic anemometer and two condensation particle counters was set up and successfully applied above a Norway spruce forest in NE Bavaria, Germany. Particle deposition clearly dominated over emission, with the strongest deposition fluxes occurring during particle formation events identified from submicron particle size distributions. Typical deposition velocities derived from these measurements ranged from - 37 to + 23 mm s⁻¹. The ultrafine particle fraction (3 – 11 nm diameter) showed different concentration patterns and larger deposition velocities as compared to the particle fraction with larger diameters. Also, particle deposition occurring before noon could be attributed mainly to the ultrafine particle fraction, whereas larger particles contributed to turbulent deposition in the afternoon.

INTRODUCTION

Vertical exchange of gases and particles between the surface and the boundary layer is mainly established through atmospheric turbulence. Quantitative knowledge about this turbulent exchange is a key prerequisite to understand ecosystem budgets of nutrients and pollutants. It is also fundamental for the dynamics of aerosol populations and their effect on atmospheric properties and processes. However, the quantification of turbulent exchange, especially of particles, is complex and still a challenging endeavor (Wesely and Hicks, 2000). Various approaches have been suggested to measure and estimate particulate fluxes between the atmosphere and the surface. One straightforward direct approach is sampling and analyzing particles on surrogate surfaces (e.g. Franz *et al.*, 1998). In most cases, a large disadvantage of this method is the rather poor imitation of the real deposition surface and flow regime. Atmospheric deposition of gases and particles above forest stands is commonly determined by comparison of bulk precipitation and throughfall measurements (e.g. Matzner *et al.*, 2004). This method is limited by unaccounted canopy processes affecting the measured fluxes. The “gradient” method (e.g. Fowler *et al.*, 2001) is another widely used indirect technique. Here, the vertical flux is calculated as the product of the measured vertical concentration gradient and the so-called eddy diffusivity which is estimated from proxy measurements. However, in a well-developed turbulence regime, only small gradients are established, thus limiting the gradient method depending on the quality of the chemical analysis system. In the inferential approach, the deposition flux F is calculated as the product of the measured scalar concentration, c , and the so-called deposition velocity, v_d ,

$$F = -v_d \cdot c. \quad [\text{Eq. 1}]$$

The deposition velocity combines all micro-physical mechanisms contributing to the dry deposition in a single parameter. For this reason, the quality of the inferential approach depends mainly on the parameterization of the deposition velocity.

Direct micrometeorological approaches such as the “eddy covariance” (EC) or the “eddy accumulation” (EA) methods (e.g. Stull, 2000) yield promising results, however, in contrast to many gaseous species, the application of these techniques to particle flux measurements is still a field of research. Relaxed eddy accumulation (REA) has been applied to measure particle fluxes in a semi-arid environment (Schery et al., 1998), in an urban environment (Nemitz et al., 2001), and for size-resolved measurements (Gaman et al., 2004).

The vertical particle number flux may be directly measured by eddy covariance. In this approach, particle number concentrations and the vertical wind velocity are measured with high time resolution in order to obtain the mean value and the turbulent fluctuations of these scalars. Thus, the turbulent flux may be calculated as the covariance of the particle concentration and the vertical wind velocity.

Fluctuations of the vertical wind are routinely measured using sonic anemometers with time resolutions of 10 – 20 Hz. Atmospheric particles may be detected using electrical or optical counters. Flux experiments using electrical counting devices were limited to particle sizes > 100 nm diameter (e.g. Lamaud et al., 1994). Early studies using optical particle counters in eddy covariance systems were limited by the slow response of the instruments (Katen and Hubbe, 1985; Duan et al., 1988). Nevertheless, recent work by Gallagher et al. (1997) and Nilsson et al. (2003) yielded interesting results for high particle concentrations. Optical counting of individual particles due to light scattering is also limited to particles > 100 nm diameter. Below this threshold, the scattering intensity becomes too small to be detected (Flagan, 1998).

The BEWA joint project within the German atmospheric research programme AFO2000, however, aimed to study the role of biogenic volatile organic compounds and their reaction products in particle formation processes (Steinbrecher et al., 2004). When studying atmospheric particle formation it is essential to use particle counters with detection limits below 100 nm diameter. This led to the use of condensation particle counters in eddy

covariance systems (Buzorius et al., 1998). In this work, an eddy covariance system combining a sonic anemometer and two condensation particle counters was set up and applied above a Norway spruce forest. In particular, the turbulent vertical fluxes of aerosol particles during particle formation events were investigated. The identification and analysis of particle formation events from particle size distribution measurements are presented in Held et al. (2004). Here we describe the BEWA particle flux system, and present results of the particle flux measurements during the BEWA field campaigns.

METHODS

Site

The BEWA field campaigns were carried out in July/August 2001 and 2002, respectively, at the “Waldstein” ecosystem research site of the Bayreuth Institute of Terrestrial Ecosystem Research (BITÖK) in the “Fichtelgebirge” mountain range. This forest site situated near the Czech/German border ($50^{\circ}09'N$, $11^{\circ}52'E$) is dominated by Norway spruce (*Picea abies* (L.) Karst) surrounding a 30 m scaffolding tower at 776 m asl. In recent years, both eddy covariance (e.g., Klemm and Mangold, 2001; Burkard et al., 2002; Rebmann et al., 2004) as well as eddy accumulation techniques (e.g. Pryor and Klemm, 2004) were successfully applied over the heterogeneous terrain of the “Fichtelgebirge” mountains at this site. Footprint analyses indicate that source areas contributing to turbulent fluxes are covered with Norway spruce in most cases except for very stable conditions (Klemm and Mangold, 2001). Further details may be found in Klemm et al. (this issue) and Matzner (2004).

Instrumentation

An eddy covariance system (Fig. 1) for turbulent particle flux measurements was set up combining a Young Model 81000 sonic anemometer (R.M. Young, Traverse City, MI, USA) and two condensation particle counters, a CPC 3760A (CPC) and a UCPC 3025 (UCPC; both TSI Inc., St. Paul, MN, USA).

→ Fig. 1

The sonic anemometer and the CPC were mounted on a swinging boom at 22 m agl approximately 3 m from the SE corner of a 30 m scaffolding tower surrounded by a Norway spruce stand. The UCPC, the data acquisition and control PC as well as auxiliary parts of the system (pumps, power supply, electronics) were located on the 21 m tower platform.

In both the CPC and the UCPC, the aerosol sample passes a convectively heated saturation chamber with an oversaturated butanol atmosphere. The butanol vapor condenses onto the particles downstream in the condensation chamber. Subsequently, the grown particles are individually counted by optical detection of laser light scattering. The particle growth depends on the internal design of the counter, on the temperature difference between the saturator and the condenser and also on the flow rate through the counter. The temperature difference between the saturator and the condenser was maintained at 17 K in 2001 and 22 K in 2002 for the CPC and at 28 K for the UCPC, respectively. With an external pump (N815 KNE, KNF Neuberger, Freiburg, Germany) and a critical orifice a 1.5 l min^{-1} flow rate and sample flow through the CPC was set. The UCPC was operated at a flow rate of 1.5 l min^{-1} , however, the sample flow through the UCPC was only 0.03 l min^{-1} .

The minimum detectable particle size of the counter is usually defined as the smallest diameter of particles detected with an efficiency of 50 %. In general, the 50 % detection efficiency decreases with increasing temperature differences and decreasing flow rates. The 50 % detection limit of the CPC is around 11 nm, the 50 % detection limit of the UCPC around 3 nm (TSI, 1989; TSI, 1998). It is important to bear in mind that the variation of the temperature difference or the flow rate will not only change the 50 % detection limit of the counter but will rather change the functional relationship of the counter's detection efficiency for different particle sizes (Mertes et al., 1995).

Particles were sampled near the sonic anemometer's measuring region and were transported to the particle counters through conductive tubing. The dimensions of the sampling lines can be found in Tab. 1.

→ Tab. 1

A standard PC was used for system control, data acquisition and data storage. The three-dimensional wind vector and the sonic temperature data were acquired from the sonic anemometer via serial communication with a time resolution of 10 Hz. The CPC and UCPC data were fed into electronic counting boxes (elub 0661, Universität Bayreuth, Germany) counting the detection pulses of each individual particle with a fixed time resolution of 10 Hz.

Analysis

The above system yields horizontal and vertical wind velocity data, sonic temperature and particle number concentrations in the size range from 3 nm to $> 3 \mu\text{m} \varnothing$ (c_{UCPC}) and from 11 nm to $> 3 \mu\text{m} \varnothing$ (c_{CPC}), respectively. The particle concentration for the ultrafine size fraction from 3 to 11 nm \varnothing (c_{UF}) may be easily determined as the difference of c_{UCPC} and c_{CPC} . However, the exact ultrafine size range depends on the specific 50 % detection efficiency of the used counters which has not been calibrated. Particle concentrations were corrected for coincidence using the correction as given by the manufacturer (TSI, 1998). Also, particle losses in the sampling lines due to gravitational settling and diffusive deposition were taken into account applying correction factors acc. Willeke and Baron (1996). This correction ranged from 4 to 12 % for the different sampling setups.

Turbulent fluxes of buoyancy, momentum and particles were determined by the eddy covariance (EC) method. The vertical turbulent exchange corresponds to the covariance of the vertical wind velocity w and the studied scalar x ,

$$F_x = \overline{w'x'}, \quad [\text{Eq. 2}]$$

with x being temperature T , horizontal wind speed u , or particle concentration c . Large eddies contributing to the turbulent flux were taken into account by using 30-min averaging intervals. An analysis of ogive functions (e.g. Friehe et al., 1991) showed that this was an adequate interval for the BEWA flux measurements.

Wind and particle concentration data were synchronized, i.e., they were corrected for the time lag introduced due to the particle sampling lines, by maximizing the covariance given by the cross correlation function of vertical wind and particle concentration. Using theoretically calculated travel times of the particles to the counter, the cross correlation procedure was limited to a plausible range of time lag values.

The vertical orientation of the sonic anemometer was corrected by application of a planar-fit coordinate rotation (Wilczak et al., 2001). This procedure adapts the wind measurements to the mean streamlines over the terrain around the measuring tower.

Also, before flux calculation the data were detrended by subtracting a 200-s moving average from the original time series. This procedure was used to separate the true turbulent signal from low frequency contributions that may be introduced, e.g., due to changing meteorological conditions.

After synchronization, coordinate rotation and detrending, the buoyancy flux, the momentum flux and the turbulent particle fluxes for the CPC and the UCPC measurements were calculated.

Finally, rigorous quality tests were carried out to identify and filter reliable flux data. The valid application of the eddy covariance method requires theoretical assumptions such as the stationarity of the time series. This was tested acc. Foken and Wichura (1996) by comparison of 30-min dispersions and the average of six 5-min dispersions of the same interval. 30-min intervals exhibiting differences smaller than 30 % were considered stationary in this study. After detrending of the time series as described above only 0.2 % of the data had to be excluded as not stationary.

Two criteria for well-developed turbulence were investigated: If the friction velocity u_* (calculated as the square root of the negative momentum flux, $\sqrt{-\overline{w'u'}}$) was below a threshold value of 0.1 m s^{-1} , the data were discarded. Also, the so-called integral turbulence characteristic (Thomas and Foken, 2002) of the vertical wind was evaluated and compared

with a theoretical model. Again, for differences between observation and model larger than 30 %, data were assigned a low-quality status. Under northerly wind conditions, the wind field is distorted due to the measuring tower construction thus degrading the flux measurements. Therefore, only measurements in the wind sector from 120° to 300° were considered for data analysis. Overall, 852 of 1615 acquired 30-min intervals (53 %) passed all quality tests and were included in the data analysis.

The general applicability of the setup for eddy covariance measurements was investigated by spectral analysis (Kaimal and Finnigan, 1994) of the vertical wind velocity and particle concentration time series. At high frequencies (> 1 Hz), deviations of the CPC particle power spectra from the ideal spectral model were observed. A slope of +1 indicated white noise at high frequencies, i.e., fluctuations faster than ~ 1 Hz could not be resolved with the CPC. This limitation is not only due to the slow response of the particle counter, but also due to the sampling line setup. In order to take into account the fluctuation damping, the time response of the CPC and the UCPC together with their respective sampling line configuration were experimentally determined and used in a simple spectral correction model (Horst, 1997). Particle concentration step changes were created using a magnetic valve switching between ambient air and filtered, particle-free air. The response of the CPC and the UCPC systems was recorded, respectively, and the time constants were determined by fitting a theoretical exponential function with the experimental data (Buzorius, 2001),

$$\frac{c_0(t)}{c_i(t)} = \exp\left(-\frac{t-t_0}{\tau}\right), \quad [\text{Eq. 3}]$$

c_0 , true concentration signal [m^{-3}], c_i , measured concentration signal [m^{-3}], t_0 , time of the concentration step [s], τ , response time [s].

→ Fig. 2

As an example, the averaged response (10 repetitions) of the CPC setups 2001 and 2002 and the corresponding theoretical response functions are displayed in Fig. 2. Evidently, the

theoretical function seems to be a proper representation of the actual CPC response, i.e., the corresponding response times $\tau = 0.96$ s (2001) and $\tau = 0.77$ s (2002) may be used to correct the system attenuation. Due to the longer sampling lines, a considerably slower response of the UCPC setup was determined, with $\tau = 1.82$ s (2001) and $\tau = 0.91$ s (2002), respectively. The corresponding spectral flux corrections acc. Horst (1997) were typically on the order of 10 % to 20 %. In 2001, the UCPC flux corrections reached 40 % in some cases, however, in 2002, less than 5 % of the measurements needed corrections greater than 20 %.

RESULTS AND DISCUSSION

Vertical turbulent fluxes of aerosol particles were measured above a Norway spruce forest using an eddy covariance system. The particle counters measured particle concentrations over a wide size range from a few nm to several μm . Thus, the resulting flux measurements yield integral number fluxes of the polydisperse particle population.

→ Fig. 3

Fig. 3 shows six days of turbulent particle number fluxes as measured with the CPC and the UCPC systems, respectively. The CPC and UCPC flux patterns are quite similar to each other. Even small features of the flux pattern can be observed in both measurements. However, the absolute value of the UCPC flux is generally higher than that of the CPC flux. This is due to the different lower detection limits of the two counters.

Both measurements exhibit a clear diurnal variation with negligible fluxes during night-time and stronger fluxes during the day. In most cases, the daytime fluxes are negative, i.e., the turbulent particle fluxes are directed towards the surface. These deposition fluxes dominate over emission fluxes which occurred only episodically during the field experiments (Fig. 4)

→ Fig. 4

In the CPC measurements, small deposition fluxes up to $-5 \cdot 10^6$ particles $\text{m}^{-2} \text{s}^{-1}$ were observed most frequently. About 85 % of the CPC fluxes were found in the range from $-25 \cdot 10^6$ to $+5 \cdot 10^6$ particles $\text{m}^{-2} \text{s}^{-1}$. Emission fluxes could be observed in 122 intervals (14 %) whereas

deposition occurred during 730 intervals (86 %). The frequency distribution of the UCPC fluxes is clearly shifted towards negative fluxes with 788 deposition measurements (92 %) vs. 64 emission measurements (8 %). About 81 % of the flux measurements were in the range from $-35 \cdot 10^6$ to $+5 \cdot 10^6$ particles $\text{m}^{-2} \text{ s}^{-1}$.

The day-to-day variability of the particle fluxes becomes evident in a compilation of daily median and 90 % percentile values of all campaign days with more than 25 % of high quality data coverage in Fig. 5.

→ Fig. 5

The fraction of deposition and emission fluxes, respectively, as well as the low quality data fraction is displayed in the upper panel of Fig. 5. Again, the dominance of particle deposition over emission (black vs. grey filling) becomes evident. The absolute daily median values of the CPC deposition flux are typically below $10 \cdot 10^6$ particles $\text{m}^{-2} \text{ s}^{-1}$, and reach a maximum of $39 \cdot 10^6$ particles $\text{m}^{-2} \text{ s}^{-1}$ on July 27, 2002. The 90 % percentile is a robust estimate of the maximum deposition flux and exceeds an absolute value of $30 \cdot 10^6$ particles $\text{m}^{-2} \text{ s}^{-1}$ on eight days (marked “F” in Fig. 5). These “deposition” days also exhibit the highest UCPC fluxes (not shown) with more than $50 \cdot 10^6$ particles $\text{m}^{-2} \text{ s}^{-1}$. Significant emission fluxes were only observed on four days. Neglecting particle deposition, the maximum median value of particle emission (not shown) was $125 \cdot 10^6$ particles $\text{m}^{-2} \text{ s}^{-1}$ on July 30, 2002.

The concentration and flux differences between the CPC and the UCPC system can be attributed to the particles that are measured with the UCPC but not with the CPC, i.e. the ultrafine particle fraction (UFP) from 3 nm to 11 nm diameter. In the case of particle concentration it is straightforward to calculate the difference to obtain the UFP concentration, however, for particle fluxes it is almost impossible to take into account all differences of the counter properties affecting the eddy covariance measurement (Buzorius et al., 2003). Nevertheless, it is an instructional effort to compare the differential flux (called UFP flux)

with the respective CPC and UCPC fluxes. Tab. 2 gives typical values of particle concentrations and particle deposition fluxes during the BEWA campaigns 2001 and 2002.

→ Tab. 2

While the concentration difference yields an UFP fraction of typically much less than 25 %, the contribution of the ultrafine particles to the overall deposition flux is frequently on the order of 50 % or more. These results emphasize the large impact of ultrafine particles on the particle number flux, especially during so-called nucleation events when new particles are formed in the atmosphere through gas-to-particle conversion. In a coniferous forest, oxidation products of biogenic volatile organic compounds such as monoterpenes and sesquiterpenes contribute to particle growth through condensation and possibly also to new particle formation (e.g. Kavouras et al., 1998). These newly formed particles can be detected at sizes of several nanometers in diameter. In this size range, particle deposition models (e.g. Zhang et al., 2001) predict decreasing deposition velocities with increasing particle size, i.e. small particles should exhibit large deposition velocities. Thus, the large abundance of ultrafine particles is very likely to result in strong deposition fluxes during nucleation events. This assumption has been confirmed during the BEWA field campaigns. For example, six of the eight days with strong particle deposition (cf. Fig. 5) could be classified as particle nucleation event days (Held et al., 2004). If particles were formed within the forest stand, their emission was not detected by the flux system because particle growth was probably too slow to produce particles larger than 3 nm within the forest stand.

A remarkable observation was made on July 12, 2002, when measurements showed strong particle exchange during a pronounced particle formation event. On this particular day, the CPC and UCPC measurements revealed opposite particle flux directions. As displayed in the upper panel of Fig. 6, particle emission was measured with the CPC system while the UCPC system showed particle deposition.

→ Fig. 6

In order to elucidate this special situation, the time evolution of the particle number concentrations is shown in the lower panel of Fig. 6. From the measurements, the concentration of three particle fractions, i.e. the UCPC size range, the CPC size range and the UFP fraction, were derived. The UFP fraction is the difference between UCPC and CPC, and thus, UCPC is the sum of CPC and UFP, i.e., the total particle concentration. As expected, the total concentration increases in the morning hours reaching a morning maximum of 23 000 particles cm^{-3} between 09:30 and 10:00 CET and a second, less pronounced peak between 12:00 and 13:00 CET. While the UFP fraction follows the UCPC concentration pattern over the whole day, the CPC concentration shows a somewhat different evolution. The CPC concentration increases slowly and continuously over the morning hours until it reaches its maximum between 12:00 and 13:00 CET. Thus, it is reasonable to attribute the steep concentration increase and the morning maximum of the total concentration to the UFP fraction. This fraction also dominates the UCPC flux measurements in the morning hours when the opposite direction of the CPC and UCPC fluxes is strongly pronounced. Therefore, the particle emission flux as measured with the CPC system is masked in the UCPC measurement due to the high deposition velocity and the large abundance of the UFP fraction, and the UFP dominance of the UCPC measurements results in a net deposition flux. Overall, the differing dynamics of the UFP and CPC fractions as apparent in the concentration patterns and their differing deposition mechanisms may lead to opposite flux directions of these fractions.

The differing evolution of these particle size fractions was observed to be a general feature of the particle dynamics during the BEWA campaigns. This is demonstrated in Fig. 7 showing the median diurnal pattern of the deposition velocities of the UCPC, CPC and UFP size fractions.

→ Fig. 7

From the direct measurement of the particle concentrations c and the fluxes F , the integral deposition velocity,

$$v_d = -\frac{F}{c}, \quad [\text{Eq. 4}]$$

was calculated for the three fractions. As expected from theoretical particle deposition models, the UFP deposition velocity is typically larger than the integral deposition velocities of the CPC and UCPC fractions. The contribution of larger particles with lower deposition velocities decreases the integral deposition velocities of both the CPC and the UCPC system. The UFP deposition velocity peaks in the morning around 11:00 CET, whereas the CPC deposition velocity shows a maximum later in the day around 15:00 CET. The UCPC deposition velocity, in contrast, exhibits two peaks, one before noon and one in the mid-afternoon. Apparently, the UCPC pattern is a superposition of the complementing UFP and CPC fractions. The morning peak may be attributed to the ultrafine particles which are produced early in the morning during particle formation events. In contrast, the afternoon peak is mainly due to particles larger than 11 nm \varnothing (CPC) when ultrafine particles have already grown to larger sizes.

CONCLUSIONS

In this work, an eddy covariance system was set up and successfully applied above a Norway spruce forest to directly measure the vertical turbulent exchange of aerosol particles between the vegetative surface and the atmospheric boundary layer. The resulting deposition velocities on the order of 10 mm s^{-1} are consistent with values found in other studies over comparable surfaces (Tab. 3).

→ Tab. 3

Considerably lower deposition velocities have been measured above open sea and low vegetation such as crop or moorland. This is due to effective impaction and interception

processes taking place in a coniferous forest and also due to the different surface roughnesses, consequently resulting in a modified turbulence regime.

While Buzorius et al. (2001) used two CPCs of the same type and Gaman et al. (2004) used a differential mobility particle sizer, here for the first time, the simultaneous use of a CPC and a UCPC allowed to derive a direct estimate of the turbulent flux of the ultrafine particle fraction (UFP) in the size range from ~ 3 to ~ 11 nm diameter. The measured UFP deposition velocity values were consistent with theoretical models. Therefore, the UFP estimates may be considered reliable, and thus, may be used in a comparison of the UFP vs. CPC particle dynamics. The differences in the diurnal behavior of these two particle fractions need to be considered when analyzing deposition processes and the evolution of an atmospheric particle population. For a better understanding of the atmospheric aerosol dynamics, size resolved particle fluxes are desirable. Therefore, a rigorous measurement of the turbulent particle flux would determine particle fluxes of various size ranges individually. However, the development of sufficiently fast instrumentation for this task and successful implementation in an eddy covariance system remains a future challenge in atmospheric research. Ultimately, the measurement of particle mass fluxes and the exchange of chemical species in the gas and particle phases need to be tackled. We consider the presented results of the BEWA particle flux measurements a valuable step towards this goal.

ACKNOWLEDGEMENTS

We appreciate the help of T. Braun, J. Gerchau, G. Müller, T. Wrzesinsky and the support of the BEWA community. This study was funded by the German federal ministry of education and research (BMBF) through grants PT BEO 51–0339476 D (BITÖK) and PT UKF 07ATF25 (BEWA).

REFERENCES

Burkard, R., Eugster, W., Wrzesinsky, T., Klemm, O., 2002. Vertical divergences of fogwater fluxes above a spruce forest, *Atmospheric Research* **64**, 133-145.

Buzorius, G., 2001. Cut-off sizes and time constants of the CPC TSI 3010 operating at 1-3 lpm flow rates. *Aerosol Science and Technology* **35**, 577-585.

Buzorius, G., Rannik, Ü., Mäkelä, J.M., Vesala, T., Kulmala, M., 1998. Vertical aerosol particle fluxes measured by eddy covariance technique using condensational particle counter. *Journal of Aerosol Science* **29**, 157-171.

Buzorius, G., Rannik, Ü., Mäkelä, J.M., Keronen, P., Vesala, T., Kulmala, M., 2000. Vertical aerosol fluxes measured by the eddy covariance method and deposition of nucleation mode particles above a Scots pine forest in southern Finland. *Journal of Geophysical Research* **105**, 19905-19916.

Buzorius, G., Rannik, Ü., Nilsson, E.D., Kulmala, M., 2001. Vertical fluxes and micrometeorology during aerosol particle formation events. *Tellus* **53B**, 394-405.

Buzorius, G., Rannik, Ü., Nilsson, E.D., Vesala, T., Kulmala, M., 2003. Analysis of measurement techniques to determine dry deposition velocities of aerosol particles with diameters less than 100 nm. *Journal of Aerosol Science* **34**, 747-764.

Dorsey, J.R., Nemitz, E., Gallagher, M.W., Fowler, D., Williams, P.I., Bower, K.N., Beswick, K.M., 2002. Direct measurements and parameterisation of aerosol flux, concentration and emission velocity above a city. *Atmospheric Environment* **36**, 791-800.

Duan, B., Fairall, C.W., Thomson, D.W., 1988. Eddy correlation measurements of the dry deposition of particles in wintertime. *Journal of Applied Meteorology* **27**, 642-652.

Flagan, R.C., 1998. History of electrical aerosol measurements. *Aerosol Science and Technology* **28**, 301-380.

Foken, T., Wichura, B., 1996. Tools for quality assessment of surface-based flux measurements. *Agricultural and Forest Meteorology* **78**, 83-105.

Fowler, D., Coyle, M., Flechard, C., Hargreaves, K., Nemitz, E., Storeton-West, R., Sutton, M., Erisman, J.W., 2001. Advances in micrometeorological methods for the measurement and interpretation of gas and particle nitrogen fluxes. *Plant and Soil* **228**, 117-129.

Franz, T.P., Eisenreich, S.J., Holsen, T.M., 1998. Dry deposition of particulate polychlorinated biphenyls and polycyclic aromatic hydrocarbons to Lake Michigan. *Environmental Science and Technology* **32**, 3681-3688.

Friehe, C.A., Shaw, W.J., Rogers, D.P., Davidson, K.L., Large, W.G., Stage, S.A., Crescenti, G.H., Khalsa, S.J.S., Greenhut, G.K., Li, F., 1991. Air-sea fluxes and surface layer turbulence around a sea surface temperature front. *Journal of Geophysical Research* **96**, 8593-8609.

Gallagher, M.W., Beswick, K.M., Duyzer, J., Westrate, H., Choularton, T.W., Hummelshoj, P., 1997. Measurements of aerosol fluxes to Speulder forest using a micrometeorological technique. *Atmospheric Environment* **31**, 359-373.

Gallagher, M.W., Nemitz, E., Dorsey, J.R., Fowler, D., Sutton, M.A., Flynn, M., Duyzer, J., 2002. Measurements and parameterizations of small aerosol deposition velocities to grassland, arable crops, and forest: Influence of surface roughness length on deposition. *Journal of Geophysical Research* **107**, doi: 10.1029/2001JD000817.

Gaman, A., Rannik, Ü., Aalto, P., Pohja, T., Siivola, E., Kulmala, M., Vesala, T., 2004. Relaxed eddy accumulation system for size-resolved aerosol particle flux measurements. *J. Atmos. Oceanic Tech.* **21**, 933-943.

Held, A., Nowak, A., Birmili, W., Wiedensohler, A., Forkel, R., Klemm, O., 2004. Observations of particle formation and growth in a mountainous forest region in Central Europe. *J. Geophys. Res.* **109**, D23204, doi:10.1029/2004JD005346.

Horst, T.W., 1997. A simple formula for attenuation of eddy fluxes measured with first-order-response scalar sensors. *Boundary-Layer Meteorology* **82**, 219-233.

Kaimal, J.C., Finnigan, J.J., 1994. Atmospheric boundary layer flows: Their structure and measurement. Oxford University Press, New York, 289 pp.

Katen, P.C., Hubbe, J.M., 1985. An evaluation of optical particle counter measurements of the dry deposition of atmospheric aerosol particles. *Journal of Geophysical Research* **90**, 2145-2160.

Kavouras, I.G., Mihalopoulos, N., Stephanou, E.G., 1998. Formation of atmospheric particles from organic acids produced by forests. *Nature* **395**, 683-686.

Klemm, O., Mangold, A., 2001. Ozone deposition at a forest site in NE Bavaria. *Water, Air and Soil Pollution: Focus* **1**, 223-232.

Klemm et al. (this issue) Experiments on forest/atmosphere exchange: Climatology and fluxes during two summer campaigns in NE Bavaria.

Lamaud, E., Brunet, Y., Labatut, A., Lopez, A., Fontan, J., Druilhet, A., 1994. The Landes experiment: Biosphere-atmosphere exchanges of ozone and aerosol particles above a pine forest. *Journal of Geophysical Research* **99**, 16511-16521.

Matzner, E. (Ed.), 2004. Biogeochemistry of forested catchments in a changing environment: a German case study. *Ecological Studies* 172, Springer, Berlin, 498 pp.

Matzner, E., Zuber, T., Alewell, C., Lischeid, G., Moritz, K., 2004. Trends in deposition and canopy leaching of mineral elements as indicated by bulk deposition and throughfall measurements. In: Matzner, E. (Ed.) Biogeochemistry of forested catchments in a changing environment: a German case study. Springer, Berlin, 233-250.

Mertes, S., Schröder, F., Wiedensohler, A., 1995. The particle detection efficiency curve of the TSI-3010 CPC as a function of the temperature difference between saturator and condenser. *Aerosol Science and Technology* **23**, 257-261.

Nemitz, E., Williams, P.I., Theobald, M.R., McDonald, A.D., Fowler, D., Gallagher, M.W., 2001. Application of two micrometeorological techniques to derive fluxes of aerosol components above a city. In: Midgley, P.M., Reuther, M., Williams, M. (Eds.) *Proceedings of EUROTRAC Symposium 2000*. Springer, Berlin, 278 pp.

Nilsson, E.D., Rannik, Ü., 2001. Turbulent aerosol fluxes over the Arctic Ocean: 1. Dry deposition over sea and pack ice. *Journal of Geophysical Research* **106**, 32125-32137.

Nilsson, E.D., Maartensson, E.M., van Ekeren, J.S., de Leeuw, G., Moerman, M., O'Dowd, C.D., 2003. The primary marine aerosol source measured by eddy correlation for particles of different size and volatility. *Abstracts of the European Aerosol Conference 2003*, S539-S540.

Pryor, S.C., Klemm, O., 2004. Experimentally derived estimates of nitric acid dry deposition velocity and viscous sub-layer resistance at a conifer forest. *Atmospheric Environment* **38**, 2769-2777.

Rannik, Ü., Petäjä, T., Buzorius, G., Aalto, P., Vesala, T., Kulmala, M., 2000. Deposition velocities of nucleation mode particles into a Scots pine forest. *Environmental and Chemical Physics* **22**, 97-102.

Rebmann, C., Anthoni, P., Falge, E., Göckede, M., Mangold, A., Subke, J.-A., Thomas, C., Wichura, B., Schulze, E.-D., Tenhunen, J., Foken, T., 2004. Carbon budget of a spruce forest ecosystem. In: Matzner, E. (Ed.) Biogeochemistry of forested catchments in a changing environment: a German case study. Springer, Berlin, 143-160.

Schery, S.D., Wasiolek, P.T., Nemetz, B.M., Yarger, F.D., Whittlestone, S., 1998. Relaxed eddy accumulator for flux measurement of nanometer-size particles. *Aerosol Science and Technology* **28**, 159-172.

Steinbrecher, R., Rappenglück, B., Hansel, A., Graus, M., Klemm, O., Held, A., Wiedensohler, A., Nowak, A., 2004. Vegetation-atmospheric interactions: The emissions of

biogenic volatile organic compounds (BVOC) and their relevance to atmospheric particle dynamics. In: Matzner, E. (Ed.) Biogeochemistry of forested catchments in a changing environment: a German case study. Springer, Berlin, 215-232.

Stull, R.B., 1999. An introduction to boundary layer meteorology. Kluwer, Dordrecht, 670 pp.

Thomas, C., Foken, T., 2002. Re-evaluation of integral turbulence characteristics and their parameterisations. 15th Conference on Turbulence and Boundary Layers, Wageningen, NL, 15-19 July 2002, American Meteorological Society, 129-132.

TSI, 1989. Model 3025 Ultrafine Condensation Particle Counter Instruction Manual Revision A, TSI Inc., St. Paul, MN, USA, 113 pp.

TSI, 1998. Model 3760A/3762 Condensation Particle Counter Instruction Manual Revision B, TSI Inc., St. Paul, MN, USA, 82 pp.

Wesely, M.L., Hicks, B.B., 2000. A review of the current status of knowledge on dry deposition. *Atmospheric Environment* **34**, 2261-2282.

Wilczak, J.M., Oncley, S.P., Stage, S.A., 2001. Sonic anemometer tilt correction algorithms. *Boundary-Layer Meteorology* **99**, 127-150.

Willeke, K., Baron, P.A., 1996. Aerosol measurement: Principles, techniques, and applications. VanNostrand Reinhold, New York, 876 pp .

Zhang, L., Gong, S., Padro, J., Barrie, L., 2001. A size-segregated particle dry deposition scheme for an atmospheric aerosol module. *Atmospheric Environment* **35**, 549-560.

FIGURE CAPTIONS

Fig. 1: Schematic representation of the eddy covariance particle flux system. Find details in the text.

Fig. 2: Experimental response curves to concentration step changes and fitted response function acc. Buzorius (2001). a) CPC setup 2001 with a time constant $\tau = 0.96$ s. b) CPC setup 2002 with a time constant $\tau = 0.77$ s.

Fig. 3: Particle number fluxes of the CPC (upper panel) and the UCPC (lower panel) system from July 9 through July 14, 2001. Black lines indicate high-quality flux data, grey lines indicate data that failed one or more quality criteria.

Fig. 4: Cumulative distribution of the relative frequency of CPC (dashed) and UCPC (solid) particle number fluxes, respectively. Negative flux values represent particle deposition, positive flux values represent particle emission.

Fig. 5: Fraction of high-quality emission (grey) and deposition (black) periods (upper panel), and the daily median and 90 % percentile value for various days of the BEWA campaigns. Days with strong deposition fluxes are marked “F”.

Fig. 6: Time evolution of the a) CPC and UCPC particle fluxes and b) of the CPC, UCPC and UFP particle concentrations on July 12, 2002. Black symbols indicate high-quality flux data.

Fig. 7: Diurnal pattern of the median integral deposition velocities of the CPC and UCPC size ranges, and of the ultrafine particle (UFP) fraction, 3 – 11 nm \varnothing for all valid measurements in 2001 and 2002.

Tab. 1: Configuration of the aerosol sampling lines for the CPC and UCPC setups in 2001 and 2002, respectively.

tubing OD / ID		conductive carbon 12.7 / 7.9 mm	stainless steel 10 / 6 mm	stainless steel 3.18 / 2.1 mm
2001	CPC	0.95 m	--	--
	UCPC	0.96 m	3.63 m	--
2002	CPC	--	--	0.94 m
	UCPC	--	--	4.73 m

Tab. 2: Characteristic values of CPC, UCPC and ultrafine particle (UFP, 3 – 11 nm \varnothing) concentrations and deposition fluxes in 2001 and 2002, respectively.

	2001			2002			unit
	median	5 %	95 %	median	5 %	95 %	
CPC concentration	5473	3167	11379	4895	1994	9880	cm^{-3}
UCPC	7336	4003	17293	6196	2973	11685	cm^{-3}
UFP concentration	1887	542	5278	1275	365	2803	cm^{-3}
CPC deposition	-6.4	-0.5	-30.5	-9.4	-1.0	-60.9	$10^6 \text{ m}^{-2} \text{ s}^{-1}$
UCPC deposition	-13.9	-2.7	-69.2	-16.7	-4.0	-92.4	$10^6 \text{ m}^{-2} \text{ s}^{-1}$
UFP deposition	-6.8	-1.0	-37.5	-5.1	-0.7	-38.3	$10^6 \text{ m}^{-2} \text{ s}^{-1}$

Tab. 3: Experimentally derived particle deposition velocities v_d for various particle size ranges and surfaces. Experimental methods include relaxed eddy accumulation (REA), eddy covariance using a condensation particle counter (EC / CPC), and eddy covariance using optical particle counters (EC / OPC).

v_d [mm s⁻¹]	size range	surface	method	source
50 ... 350	~ 1 nm	semi-arid grassland	REA	Schery et al. (1998)
4.3	50 nm	coniferous forest	REA	Gaman et al. (2004)
6 ... 7	7 – 14 nm	coniferous forest	EC / CPC&CPC	Buzorius et al. (2001)
0.1 ... 15	15 – 35 nm	coniferous forest	EC / CPC&model	Rannik et al. (2000)
-75 ... -20	> 11 nm	urban	EC / CPC	Dorsey et al. (2002)
-35 ... 10	> 11 nm	coniferous forest	EC / CPC	Buzorius et al. (1998)
5 ... 40	> 11 nm	coniferous forest	EC / CPC	Buzorius et al. (2000)
1.9	> 11 nm	open sea	EC / CPC	Nilsson and Rannik (2001)
0.7	100 – 200 nm	heathland	EC / OPC	Gallagher et al. (2002)
1.4	100 – 200 nm	arable crop	EC / OPC	Gallagher et al. (2002)
2.1	100 – 200 nm	coniferous forest	EC / OPC	Gallagher et al. (2002)
10	300 – 500 nm	coniferous forest	EC / OPC	Gallagher et al. (1997)
-39 ... 70	3 – 11 nm	coniferous forest	EC / CPC&UCPC	this work
-37 ... 23	> 3 nm	coniferous forest	EC / UCPC	this work
-12 ... 13	> 11 nm	coniferous forest	EC / CPC	this work

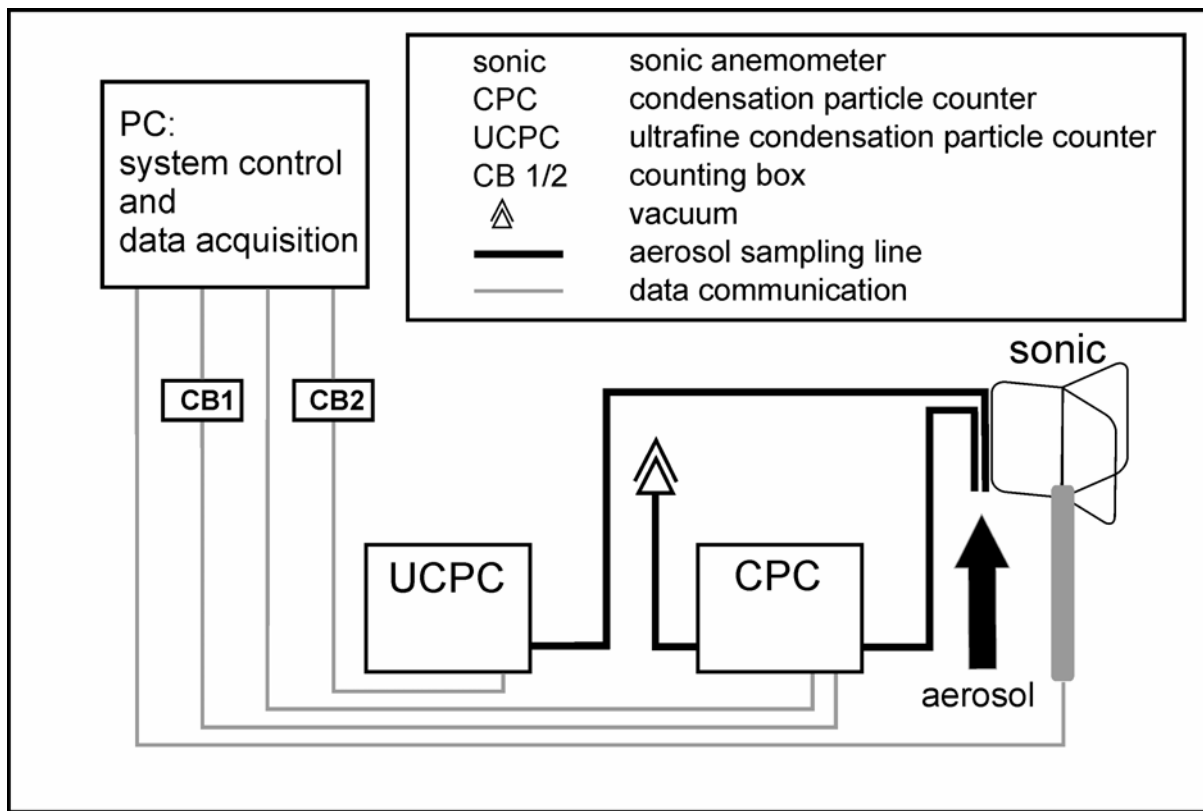


Fig. 1

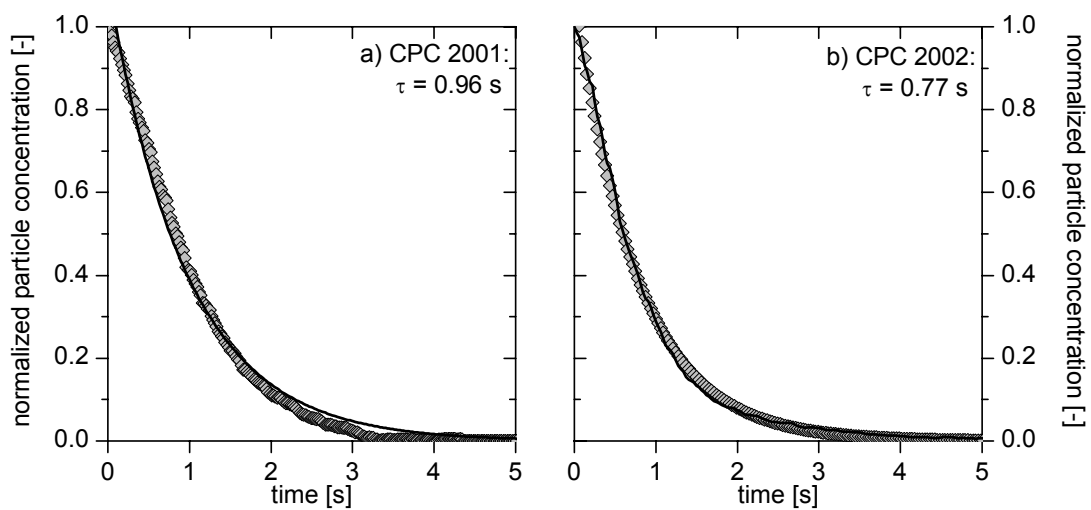


Fig. 2

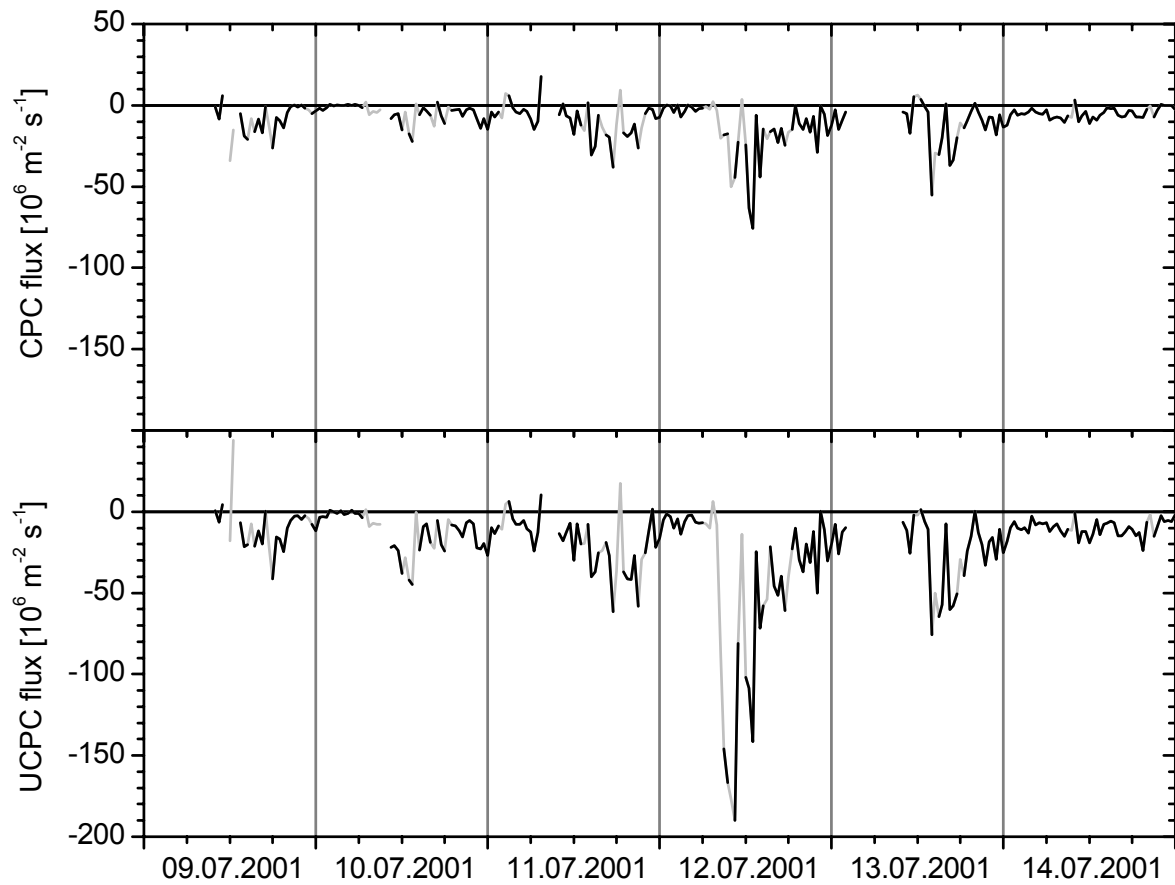


Fig. 3

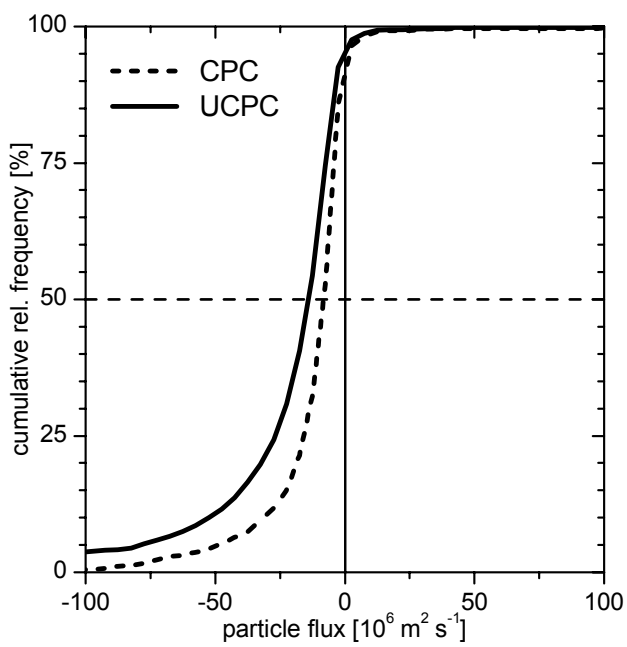


Fig. 4

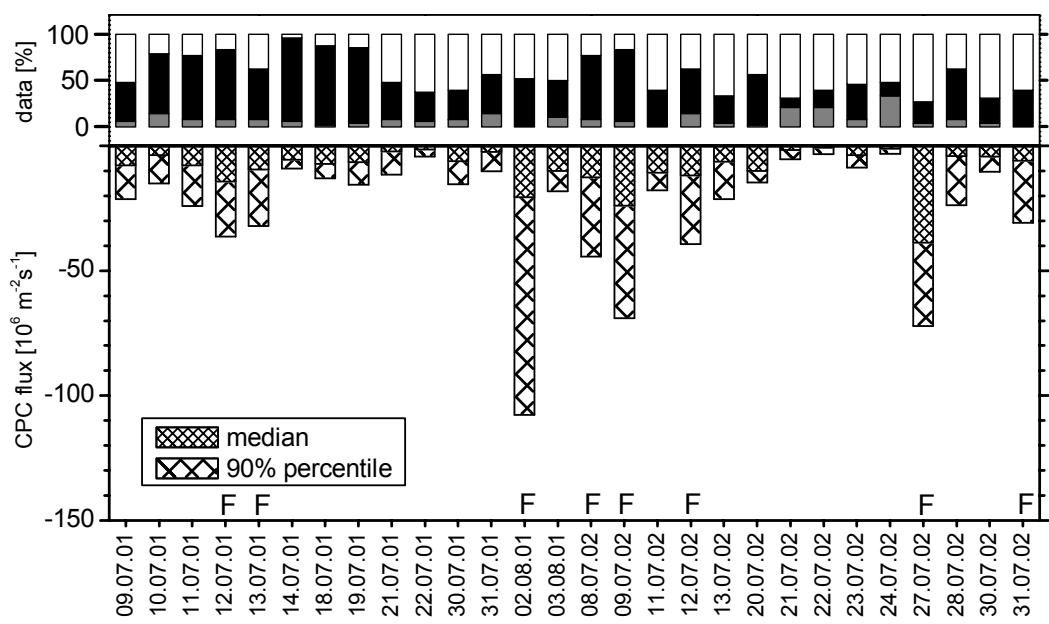


Fig. 5

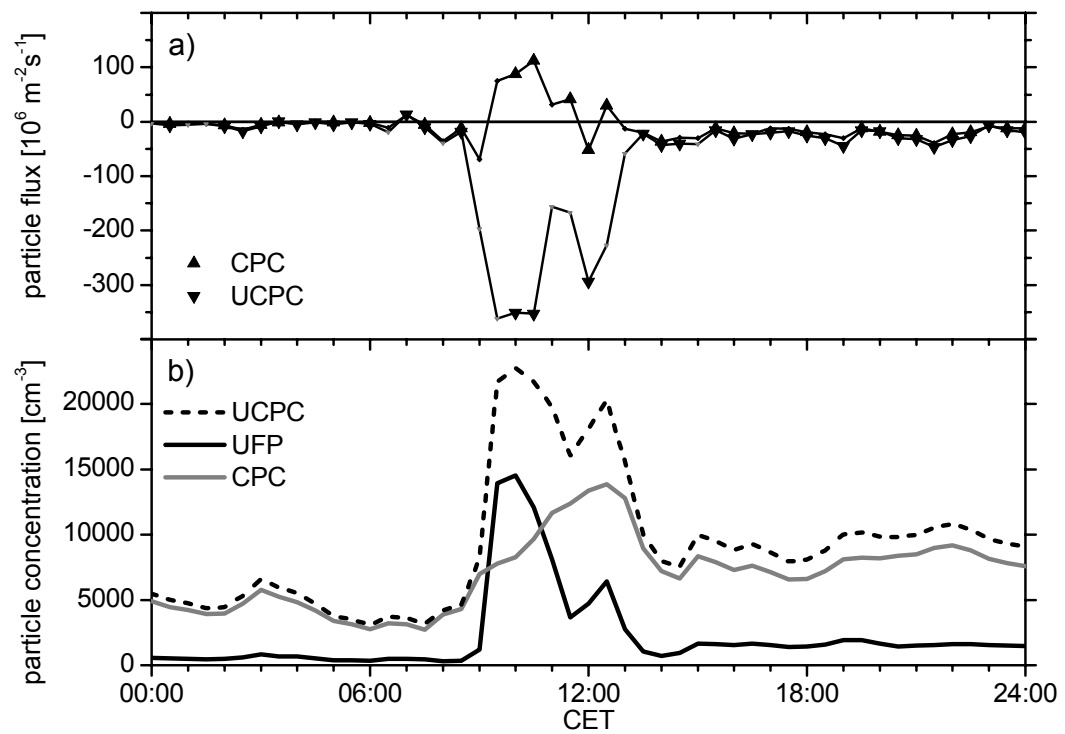


Fig. 6

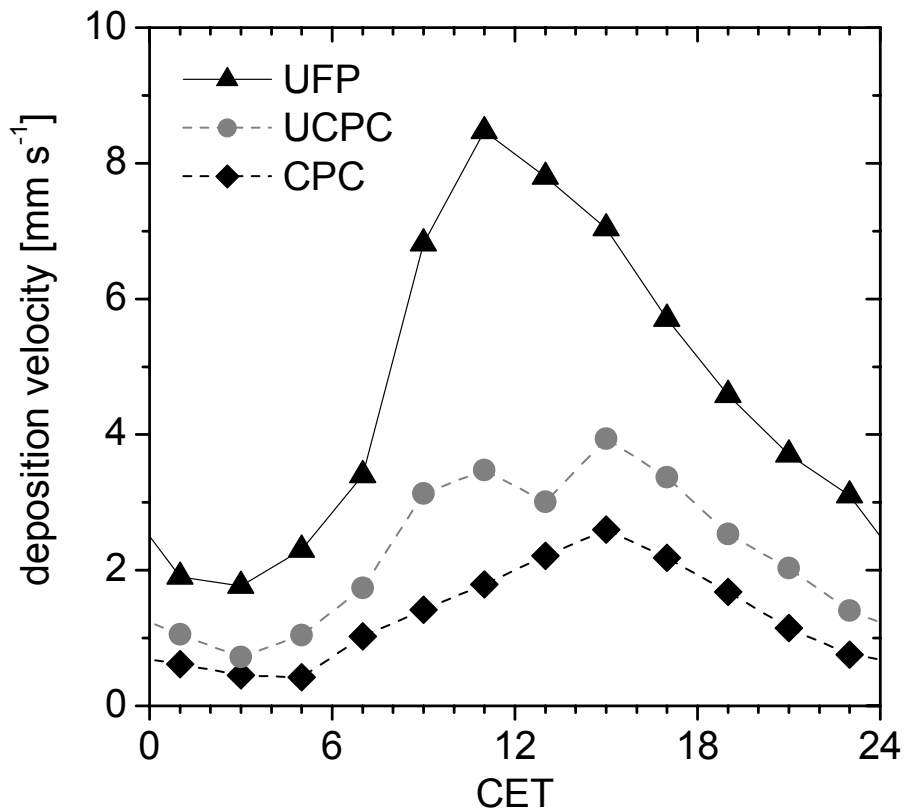


Fig. 7